

# Reference region selection and the association between the rate of amyloid accumulation over time and the baseline amyloid burden

Janusch Blautzik<sup>1</sup> · Matthias Brendel<sup>1</sup> · Julia Sauerbeck<sup>1</sup> · Sebastian Kotz<sup>1</sup> · Franziska Scheiwein<sup>1</sup> · Peter Bartenstein<sup>1</sup> · John Seibyl<sup>2</sup> · Axel Rominger<sup>1</sup> · for the Alzheimer's Disease Neuroimaging Initiative

Received: 25 October 2016 / Accepted: 24 February 2017 / Published online: 22 March 2017  
© Springer-Verlag Berlin Heidelberg 2017

**Abstract** Relative quantitative analysis of amyloid plaque burden in Alzheimer's disease (AD) patients can be reported as standardized uptake value ratio (SUVR) from positron emission tomography (PET). Here, the SUVR is the ratio of the mean amyloid radioligand retention in a composite (COMP) neocortical volume of interest (VOI) to that in a reference VOI, such as the cerebellum, brainstem (BST)/pons, or white matter (WM). Some longitudinal PET investigations show that the rate of amyloid accumulation to follow-up has an inverted U relationship with baseline amyloid SUVR relative to cerebellar or brainstem/pons reference VOIs. The corresponding association with SUVR relative to WM is unknown. To test the possible benefits of WM normalization, we analyzed [<sup>18</sup>F]-AV45 PET data from 404 subjects in the AD Neuroimaging Initiative (ADNI) database at baseline and 2-year follow-up (144 cognitively normal controls, 225 patients with mild cognitive impairment, and 35 AD patients). Reference regions included subcortical WM as well as

conventional cerebellar gray matter (CBL), and BST. We tested associations between each subject's inter-session change ( $\Delta$ ) of SUVR and their baseline SUVR by applying linear, logarithmic, and quadratic regression analyses. Unscaled standardized uptake values (SUVs) were correlated between VOIs at baseline and follow-up, and within VOIs in the longitudinal run. The association between  $\Delta$ SUVR and baseline SUVR relative to WM reference was best described by an inverted U-shaped function. Correlation analyses demonstrated a high regional and temporal correlation between COMP and WM VOI SUVs. For WM normalization, we confirm that the rate of amyloid accumulation over time follows an inverted U-shaped function of baseline amyloid burden. Reference region selection, however, has substantial effects on SUVR results. This reflects the extent of covariance between SUVs in the COMP VOI and those in the various reference VOIs. We speculate that PET labeling of amyloid deposition within target regions is partially confounded by effects of longitudinal changes of cerebral blood flow (CBF) on tracer delivery. Indeed, CBF may be the leading factor influencing longitudinal SUV changes. We suggest that SUVR relative to WM may be more robust to changes in CBF, and thus fitter for sensitive detection of amyloid accumulation in intervention studies.

Data used in preparation of this article were obtained from the Alzheimer's Disease Neuroimaging Initiative (ADNI) database (adni.loni.usc.edu). As such, the investigators within the ADNI contributed to the design and implementation of ADNI and/or provided data but did not participate in analysis or writing of this report. A complete listing of ADNI investigators can be found at: [http://adni.loni.usc.edu/wp-content/uploads/how\\_to\\_apply/ADNI\\_Acknowledgement\\_List.pdf](http://adni.loni.usc.edu/wp-content/uploads/how_to_apply/ADNI_Acknowledgement_List.pdf)

**Electronic supplementary material** The online version of this article (doi:10.1007/s00259-017-3666-8) contains supplementary material, which is available to authorized users.

✉ Axel Rominger  
axel.rominger@med.uni-muenchen.de

<sup>1</sup> Department of Nuclear Medicine, University of Munich, Munich, Germany

<sup>2</sup> MNI, New Haven, USA

**Keywords** Alzheimer's disease · Amyloid-PET · SUVR · Reference region · Quantification

## Introduction

Alzheimer's disease (AD) is a progressive neurodegenerative disorder that accounts for the majority of dementia cases worldwide; it is associated with the accumulation of neurofibrillary tangles and  $\beta$ -amyloid plaques in the

brain together representing the core histopathological hallmarks of AD [1]. The  $\beta$ -amyloid load of individuals with amnesic mild cognitive impairment (aMCI) and AD patients can now be selectively detected and quantified in vivo by positron emission tomography (PET) with specific amyloid binding radioligands such as [ $^{18}\text{F}$ ]-AV45 [2–4]. Both their specificity for AD pathophysiology and their sensitivity for detection of amyloidosis early in the course of the disease, and even prior to onset of overt clinical manifestations, have contributed to the burgeoning role of amyloid PET as an AD biomarker for the diagnostic work-up in clinical routine, and also in new disease-modifying intervention studies [5].

Longitudinal PET imaging of AD patients with the prototype tracer [ $^{11}\text{C}$ ]-PiB has revealed that the apparent rate of amyloid accumulation over time follows an inverted U-shaped function of the amyloid burden measured at baseline. This implies that there is an early phase of rapid amyloid deposition, which decelerates later in the course of the disease, as absolute amyloid load approaches a plateau [6, 7]. Absolute quantitation of amyloid by PET requires prolonged dynamic recordings in conjunction with arterial blood sampling. Most clinical studies assess the amyloid plaque burden in a relative quantitative approach; at some established time after tracer administration, i.e., after achieving secular equilibrium, a standardized uptake value ratio (SUVR) is determined, defined as the ratio of PET ligand retention within a cerebral gray matter volume of interest (VOI) relative to that in a reference tissue assumed to be relatively spared of amyloid plaque accumulation, so as to avoid bias. There being as yet no clear consensus, SUVR has been calculated relative to a reference VOI encompassing the whole cerebellum, as described for [ $^{18}\text{F}$ ]-florbetapir [8, 9], a CBL template for the case of [ $^{11}\text{C}$ ]-PiB [6, 7], [ $^{18}\text{F}$ ]-flutemetamol [10], and [ $^{18}\text{F}$ ]-florbetaben [11], or the brainstem (BST)/pons as reported for [ $^{11}\text{C}$ ]-PiB [12]. Recent work has suggested that the subcortical white matter (WM) presents advantages as a reference VOI for calculating SUVR in amyloid PET studies using [ $^{18}\text{F}$ ]-AV45, as WM normalization gives less variable and more accurate measurements in the longitudinal run [13, 14] with relatively low group variability [15]. Together, these properties give improved discrimination between healthy elderly, clinically ambiguous cases of aMCI, and genuine AD [15].

The inverted U-shaped association between the rate of amyloid accumulation over time and the amyloid burden at baseline examination has been documented in [ $^{11}\text{C}$ ]-PiB PET studies with SUVR calculation relative to cerebellar cortex [6, 7] and pons [12]. Since a predictable time course of amyloid accumulation is a precondition for longitudinal studies with disease-modifying treatments, it is important to establish if the inverted U-shaped time course is a general phenomenon. Therefore, we have undertaken an exploratory longitudinal study of [ $^{18}\text{F}$ ]-AV45 data with SUVR calculation relative to several reference regions, including WM.

## Methods

### Alzheimer's disease neuroimaging initiative

Data used in the preparation of this article were obtained from the Alzheimer's Disease Neuroimaging Initiative (ADNI) database (adni.loni.usc.edu). The ADNI was launched in 2003 as a public-private partnership, led by principal investigator Michael W. Weiner, MD. The primary goal of ADNI has been to test whether serial magnetic resonance imaging (MRI), PET, other biological markers, and clinical and neuropsychological assessment can be combined to measure the progression of mild cognitive impairment (MCI) and early AD. Data from ADNI-GO/-2 were included in this work. Pre-processed brain [ $^{18}\text{F}$ ]-AV45-PET images and temporally corresponding T1-weighted magnetization prepared rapid gradient echo (MPRAGE) images were downloaded from the ADNI database as available on Jan 16th, 2015. Further details are provided in the [Supplemental Information](#) (SI) section.

### Subjects

Molecular and structural longitudinal imaging data was obtained from 404 subjects from ADNI-GO and ADNI-2, as available on Jan 16<sup>th</sup>, 2015. All had undergone [ $^{18}\text{F}$ ]-AV45-PET and structural (T1-weighted MPRAGE) MRI of the brain at baseline and at a follow-up session 2 years later. The pooled study group was composed of 144 cognitively normal controls, 225 patients with aMCI, and 35 patients with AD (see Table 1 for detailed demographic data).

### Statistical analysis of demographic data

A multivariate analysis of variance (MANOVA) was performed in order to test the variables ADAS score at baseline, age, APOE4 status, length of education, and the time interval between sessions for statistical between-group comparisons; APOE4 status was scored as 1 or 2 copies of the APOE  $\epsilon$ 4 allele, or 0 (no APOE  $\epsilon$ 4 allele). Post-hoc analyses were performed with the Tukey's honest significant difference test. Fisher's exact test was applied to test between-group gender differences.

### Processing of image data

ADNI-specific [ $^{18}\text{F}$ ]-AV45-PET and MRI acquisition parameters and pre-processing steps are described in the SI section. The processing of the ADNI MRI and PET data including quality control procedures was performed as previously described in detail by Brendel et al. [15]. In brief, T1-weighted MRI data were transferred into the Montreal Neurological Institute (MNI) standard space and, after skull stripping, segmented into gray matter, WM, and cerebrospinal fluid (CSF). The segmented gray matter of each subject was subdivided

**Table 1** Demographic data of participants enrolled in the current study as stated by the ADNI database

Group	CN	MCI	AD
N (female)	144 (68)	225 (105)	35 (17)
Mean age $\pm$ SD in years	75.5 $\pm$ 6.6	71.4 $\pm$ 8.0	76.4 $\pm$ 7.4
N of APOE $\epsilon$ 4 carriers (%)	38 (26%)	98 (44%)	26 (74%)
Follow-up duration $\pm$ SD in days	727 $\pm$ 62	739 $\pm$ 82	733 $\pm$ 84
Mean ADAS $\pm$ SD at baseline	9.0 $\pm$ 4.4	13.5 $\pm$ 5.4	30.1 $\pm$ 10.8
Mean education $\pm$ SD in years	16.5 $\pm$ 2.8	16.2 $\pm$ 2.7	15.7 $\pm$ 2.8

CN: cognitively normal controls; MCI: patients with mild cognitive impairment; AD: patients with Alzheimer's disease; APOE  $\epsilon$ 4: carriers of at least one copy of the  $\epsilon$ 4 allele of the apolipoprotein gene. ADAS: Alzheimer's Disease Assessment Scale

into 83 individual supra- and infratentorial VOIs according to the atlas of Hammers [16]; individual gray matter VOIs of frontal, parietal, and temporal cortices as well as the precuneal/posterior cingulate gyrus were conjoined to form a composite (COMP) VOI, which was used for the calculation of individual standard uptake values (SUVs). Individual WM VOIs were generated by the automatic segmentation process mentioned above [15]. Each MRI-derived VOI was transferred from the MNI standard space into the native PET space of each subject by applying inverse linear and nonlinear transformations. We tested three reference regions for SUV determination, i.e., the gray matter-segmented cerebellum (CBL), the BST, and the cerebral WM. SUVs were determined by dividing the mean COMP SUV by the mean reference SUVs, thus yielding three different SUVs for each subject and session (i.e., COMP/CBL, COMP/BST, and COMP/WM). Since progressive atrophy is a potential confounder in longitudinal analyses, we implemented a partial volume effect (PVE)-corrected COMP configuration to calculate COMP\_PVEC/WM SUVs in order to adjust for possible cortical atrophy which was manifest to volumetric MRI (see SI section for further details).

### Association between $\Delta$ SUVR and baseline SUVR

The relationship between each subject's absolute inter-session change ( $\Delta$ ) of SUVR at 2-year follow-up and their own baseline SUVR was investigated by applying linear, logarithmic, and quadratic regression analyses as implemented in SPSS (SPSS Version 23, IBM SPSS Software, IBM, Armonk, NY, USA); regression analyses were applied to the SUVR data of all (404) subjects calculated with each of the three quantification methods. To normalize for minor individual deviations from the mean 730-day interval between scanning, individual changes in SUVR were scaled by the formula:

$$\Delta\text{SUVR} = \frac{(\text{SUVR follow up} - \text{SUVR baseline})}{(\text{days between baseline and follow-up})} * 730$$

In cases giving several statistically significant fits ( $p < 0.05$ ), the best fitting model was identified by applying the Akaike information criterion (AIC) [17]. Age, gender, years of education, and APOE4 status was included as covariates in the regression analyses.

In addition, we characterized the association between  $\Delta$ SUVRs and SUVRs at baseline across all quantification methods by grouping  $\Delta$ SUVRs into quartiles according to the corresponding SUVR at baseline; in so doing, we calculated the number of decliners, i.e., subjects in whom SUVR decreased from baseline to follow-up (= negative  $\Delta$ SUVRs), per baseline SUVR quartile for each quantification method. We also calculated the absolute number of negative  $\Delta$ SUVRs per method.

### SUV characteristics

A major objective of this study was to define optimal standard methods for SUVR-based quantitation of longitudinal changes in uptake of the amyloid tracer [ $^{18}\text{F}$ ]-AV45. This necessarily entails identifying the sources of bias for SUVR determination using different quantitation methods. For this purpose, we investigated the characteristics of the underlying SUVs by the following methods: First, we determined mean SUVs and the dispersion of SUV data by means of standard deviation (SD) for each VOI and session; this analysis was also performed for longitudinal %changes (% $\Delta$ ) of SUVs. Next, we correlated the baseline and follow-up COMP SUVs with those derived from the reference VOIs. In addition, we tested the relationship between % $\Delta$  SUVs derived from the COMP VOI with those derived from the reference VOIs. For all correlation analyses, we used the Pearson correlation.

### Volume analyses

Potential differences in VOI volumes of COMP, CBL, and WM across sessions were examined by applying a pairwise  $t$  test. BST volumes were not tested due to a mask-based approach for SUV extraction in this case.

### Correlations with the ADAS-Cog13

Clinical ratings included the 13-item version of the AD Assessment Scale Cognitive Subscale (ADAS-Cog13), and were downloaded from the ADNI database. Pearson correlations were calculated between ADAS-Cog13 and imaging parameters at baseline as well as in the longitudinal run.

## Results

### Demographic data

ADAS and APOE4 status significantly differed between groups ( $F[2401] = 172.20$  and  $F[2401] = 19.80$ ;  $p < 0.001$ ); age was significantly lower in MCI patients ( $71.4 \pm 8.0$  years) than in CNs ( $75.5 \pm 6.6$  years) and AD patients ( $76.4 \pm 7.4$  years;  $p < 0.001$ ). There were no statistically significant between-group differences in years of education, gender, or the inter-session time interval ( $p > 0.05$ ).

### Association between $\Delta$ SUVR and baseline SUVR

There was no significant ( $p > 0.05$ ) association between  $\Delta$ SUVR and baseline SUVR for data calculated with COMP/CBL (Fig. 1a). In the case of COMP/BST, the AIC calculation suggested that a quadratic regression was the best of the tested models for describing this association (Fig. 1b). The fitting line of the quadratic regression had an inverted U shape, meaning that  $\Delta$ SUVR (our index of amyloid deposition) accelerated in those cases with low baseline SUVR, but that this function reached a maximum, and thereafter decreased for those with baseline SUVR exceeding a certain threshold; note that the fitting line, including the 95% confidence interval (CI), was negative for cases of very high baseline SUVs, suggesting a longitudinal decrease in the amyloid burden in such individuals. Baseline SUVR level and the APOE4 status were both independent risk factors predicting SUVR changes to follow-up ( $p < 0.001$ ). The AIC also favored a quadratic fit with an inverted U shape for COMP/WM (Fig. 1c); in this case, however, the fitting line did not indicate any declines in  $\Delta$ SUVR below zero (fitting line and CI  $> 0$ ); here, only the APOE4 status was an independent risk factor for future SUVR increases ( $p < 0.001$ ).

There were no statistically significant associations between  $\Delta$ SUVR and gender or years of education for any of the quantitation methods ( $p > 0.05$ ).

We also found that the distribution of data as visualized in Fig. 1 substantially varied across quantitation methods. Data points for  $\Delta$ SUVR were more clustered within the 1<sup>st</sup> and 2<sup>nd</sup> quartiles of the corresponding baseline SUVR levels in the cases of COMP/CBL and COMP/BST (in the range of 80–91%) compared with COMP/WM (67%, Table 2). Moreover, the SUVs were more likely to show decreases over time when calculated with the combinations COMP/CBL and COMP/BST compared to COMP/WM. More specifically, there were 170 decliners for the combination COMP/CBL, 144 for COMP/BST, and 131 for COMP/WM. Relatively high numbers of decliners ( $> 50\%$ ) were found for the 4<sup>th</sup> quartile of baseline SUVs in the cases of COMP/CBL (11/17) and COMP/BST (2/2). Note in that context, that an asymmetric data set

with clustering of  $\Delta$ SUVs towards lower baseline SUVR levels in combination with a relatively high percentage of SUVR decliners at high baseline SUVs will generally favor an inverted U-shaped curve, as observed for COMP/BST. The portion of 4<sup>th</sup> quartile SUVR decliners was generally lower when WM was used for normalization (14/44, Table 2), a finding that is consistent with the observation that the fitting line in this case did not indicate any longitudinal decline of amyloid load in those subjects with initially high SUVR levels.

### SUV characteristics at baseline and follow-up

To further understand the reasons for the differences in fittings across quantitation methods, we additionally examined the underlying SUVs in more detail. We found that VOI SUVs were significantly higher for BST and WM compared to COMP both at baseline and follow-up; significantly lower results were obtained for CBL ( $p < 0.001$  each, Table 3). Dispersion of SUVs was highest for the COMP VOIs both at baseline and follow-up (19% & 20%, respectively; Table 3). Lower SUV dispersion was generally obtained for the reference VOIs, in particular for CBL (5% as opposed to 12–14% for BST and WM; Table 3). From these data, it is inferred that the impact on SUVR determination substantially differed across reference VOIs with a low impact of CBL and a substantially higher impact of BST and WM. This context is visualized in Fig. 2.

In line with the findings observed in Fig. 2, we found highly significant correlations between COMP and WM SUVs at baseline and follow-up ( $r = 0.78$ ,  $r = 0.79$ ;  $p < 0.001$ ), suggesting the presence of a coupling between these regions; correlations were also statistically highly significant ( $p < 0.001$ ) but substantially lower between COMP and CBL ( $r = 0.46$ ,  $r = 0.47$ ) and between COMP and BST ( $r = 0.36$ ,  $r = 0.37$ ).

### SUV characteristics in the longitudinal run

Longitudinal SUV changes were highest for the COMP VOI ( $2.03\% \pm 8.40\%$ ). For the reference VOIs, SUV changes—and, thus, the impact on  $\Delta$ SUVR—ranged from  $0.48\% \pm 2.72\%$  for CBL to  $0.66\% \pm 8.41\%$  for BST and  $1.07\% \pm 9.44\%$  for WM. Thus, the main impact on SUVR changes over time resulted from SUV changes within the COMP VOI. However, contribution of reference VOIs on  $\Delta$ SUVs substantially varied across quantitation methods and, in case of BST and WM, influenced  $\Delta$ SUVs to a relevant extent, as illustrated in Fig. 3.

Longitudinal SUV changes within the COMP VOI in general demonstrated moderate to high correlations with those within the reference VOIs ( $p < 0.001$ ). The highest correlations were found between COMP and WM ( $r = 0.94$ ); lower correlations existed between COMP and BST ( $r = 0.85$ ), and between COMP and CBL ( $r = 0.66$ ). These data show that  $\Delta$ SUVs from the COMP VOI were

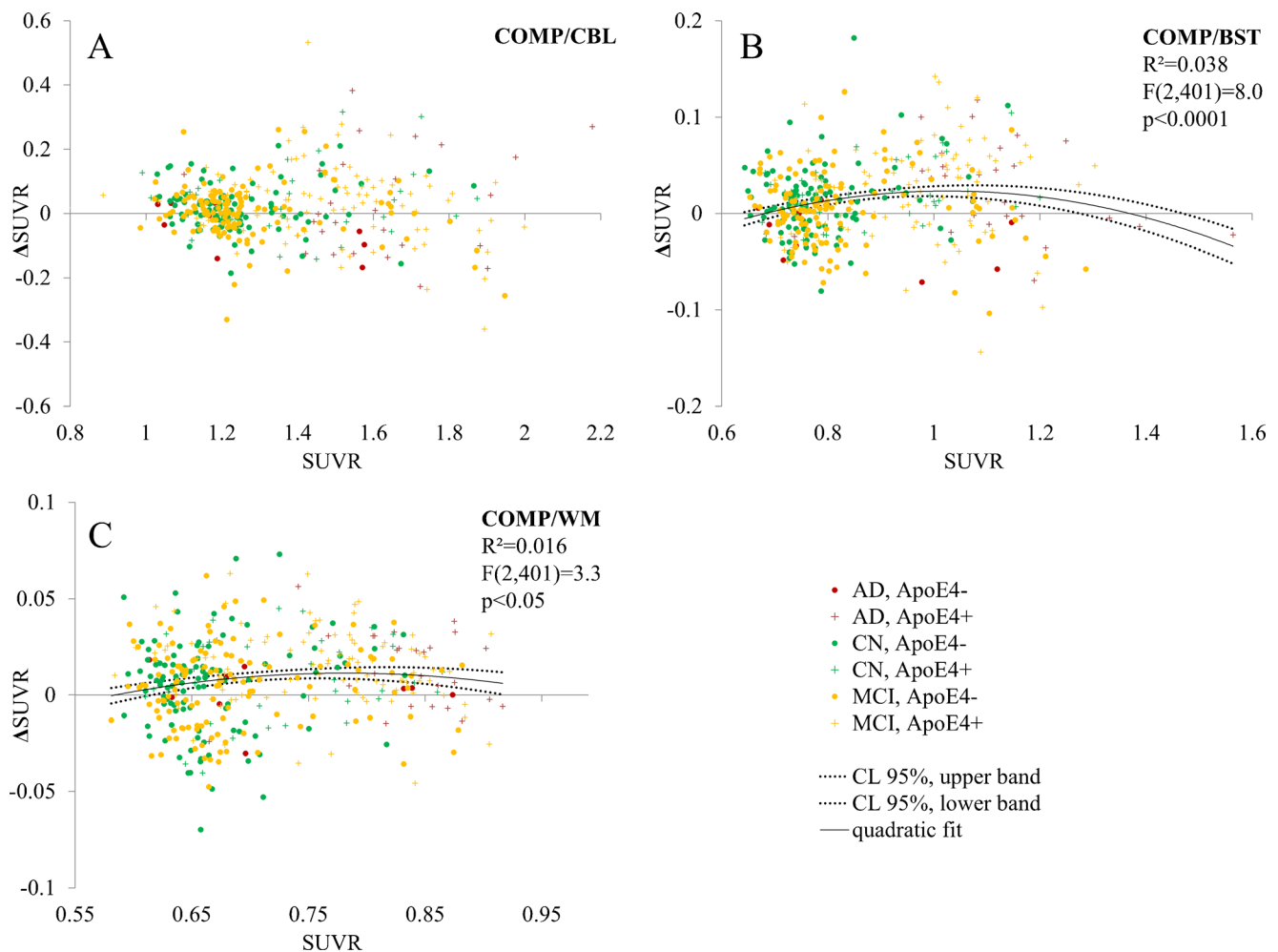


**Fig. 1** Absolute change ( $\Delta$ ) of SUVR over a 2-year period (ordinate) plotted as a function of individual baseline SUVR (abscissa) for all subjects, calculated for a composite (COMP) cerebral gray matter VOI scaled by cerebellar gray matter (CBL, **a**), brainstem (BST, **b**), and white matter segmentations (WM, **c**) as reference regions. The *solid line* represents the

best of the several fittings for COMP/BST and COMP/WM. There was no significant association between  $\Delta$ SUVR and baseline SUVR for COMP/CBL. The *dotted lines* represent the 95% confidence intervals (CI) of the regression lines

more likely to be paralleled by similar  $\Delta$ SUVs within the WM VOI compared to that within BST and CBL.

44 cm<sup>3</sup>) significantly decreased between sessions by an average of 1.66%, 1.22%, and 2.28%, respectively ( $p < 0.001$ ).

### Volume analyses

Volumes of COMP (baseline:  $482 \pm 41$  cm<sup>3</sup>; follow-up:  $474 \pm 44$  cm<sup>3</sup>), CBL (baseline:  $127 \pm 9$  cm<sup>3</sup>; follow-up:  $126 \pm 9$  cm<sup>3</sup>), and WM (baseline:  $394 \pm 42$  cm<sup>3</sup>; follow-up:  $385 \pm$

### Correlations with ADAS-Cog13

The ADAS-Cog13 data were present for all 404 subjects at baseline and for 391 subjects both at baseline and follow-up. There were highly significant correlations ( $p < 0.001$ ) between ADAS-Cog13 scores and SUVRs across all quantification

**Table 2** Distribution of  $\Delta$ SUVs across baseline SUVR quartiles

		Q1	Q2	Q3	Q4	Q1–Q4
N (%) of $\Delta$ SUVs [N of negative $\Delta$ SUVs]	COMP/CBL	150 (37%) [53]	174 (43%) [82]	63 (16%) [24]	17 (4%) [11]	404 [170, 42%]
	COMP/BST	254 (63%) [102]	112 (28%) [23]	36 (9%) [17]	2 (1%) [2]	404 [144, 36%]
	COMP/WM	161 (40%) [61]	108 (27%) [41]	91 (23%) [15]	44 (11%) [14]	404 [131, 32%]

**Table 3** Mean COMP and reference VOI SUVs ± SD at baseline and follow-up

Quantitation method	Session			
	Baseline SUV		Follow-up SUV	
	COMP VOI	REF VOI	COMP VOI	REF VOI
COMP/CBL	1.37 ± 0.26 (19%)	1.03 ± 0.05 (5%)	1.40 ± 0.28 (20%)	1.03 ± 0.05 (5%)
COMP/BST		1.60 ± 0.19 (12%)		1.60 ± 0.20 (12%)
COMP/WM		1.93 ± 0.25 (13%)		1.94 ± 0.27 (14%)

SD is given in absolute numbers and in % for the purpose of normalization across VOIs (in parentheses)

methods at baseline; the highest correlations were obtained for COMP/WM ( $r = 0.46$ ) and COMP/BST ( $r = 0.47$ ), the lowest for COMP/CBL ( $r = 0.41$ ).

In the longitudinal run, the association between imaging parameters and clinical data substantially dropped: correlations between changes ( $\Delta$ ) of ADAS-Cog13 scores and SUVRs were

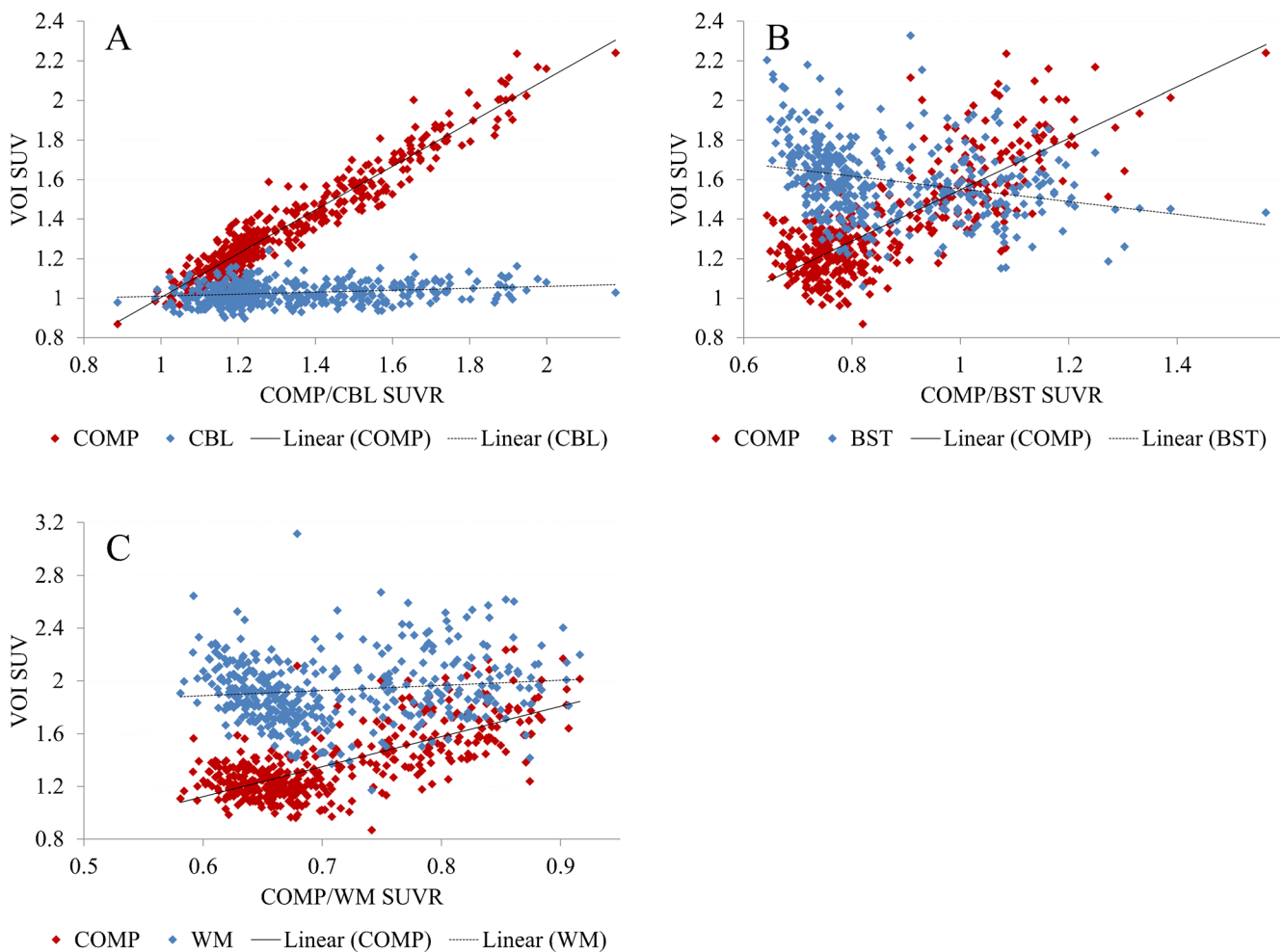


**Fig. 2** The graphs A–C demonstrate the distribution of COMP VOI SUVs and the corresponding reference VOI SUVs (ordinate) as a function of SUVr (abscissa) for each quantitation method. Data are shown for the baseline session; similar findings were obtained at 2-year follow-up (not shown here). The *solid and dotted lines* represent linear fits ( $p < 0.05$ ) of the SUV data for a simplified illustration of the association between COMP and reference VOIs. Note the differences in the impact of SUVs on SUVr determination across quantitation methods. The lowest

impact of a reference VOI (and thus the highest of the COMP VOI) was given for COMP/CBL (a). In the case of COMP/BST, there was a divergence between COMP and BST SUVs in the sense that high SUVrs were produced by high COMP SUVs and low BST VOI SUVs and vice versa (b). Higher COMP SUVs were accompanied by higher reference VOI SUVs when WM was used for normalization suggesting that WM had an attenuating effect on SUVr (c)

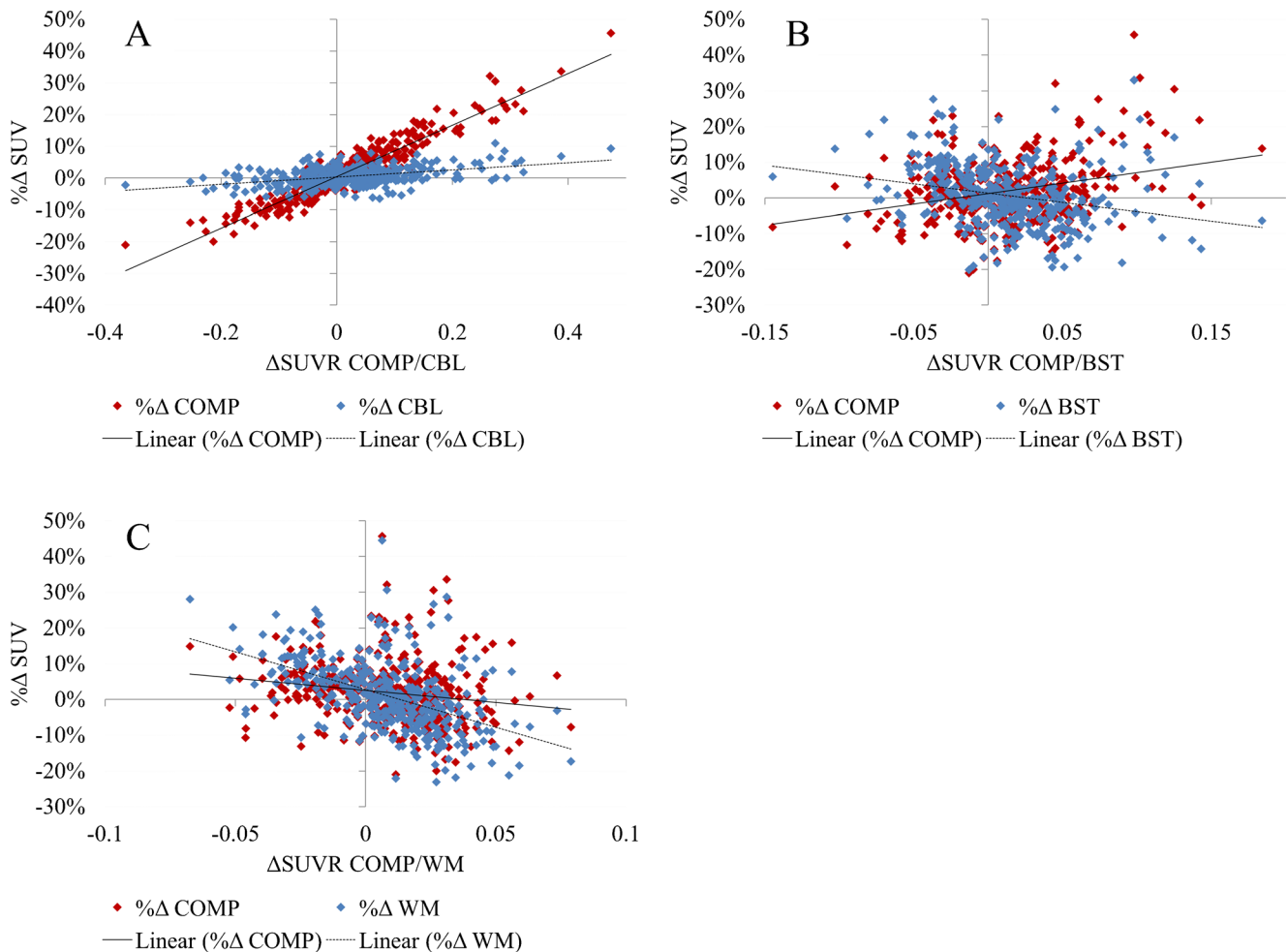


**Fig. 3** The graphs A–C illustrate the associations between % $\Delta$  COMP VOI SUVs and the corresponding % $\Delta$  reference VOI SUVs (ordinate) as a function of  $\Delta$ SUVR (abscissa) for each quantitation method. Values  $<0$  on the abscissa indicate SUVR declines between sessions, those  $>0$  SUVR incliner. The *solid and dotted lines* represent linear fits ( $p < 0.05$ ) of the % $\Delta$  SUV data and indicate the trend of SUV changes over time. Given the relative stability of CBL SUVs over time, the lowest

impact of a reference VOI (and thus the highest of the COMP VOI) on  $\Delta$ SUVR is present for COMP/CBL (a). For COMP/BST, SUV changes result from divergent SUV changes within the COMP and the reference VOI (b). In case of COMP/WM, longitudinal SUV increases predominantly result from SUV declines within the COMP VOI that are paralleled by even stronger SUV declines within the reference VOI; the opposite is true for SUV declines (c)

statistically significant for COMP/WM ( $r = 0.11$ ;  $p < 0.05$ ), but not for COMP/CBL or COMP/BST ( $r = 0.04$  each,  $p > 0.05$ ).

Results for the COMP\_PVEC/WM method are described in the SI section.

## Discussion

Recent studies have demonstrated that WM may constitute an advantageous reference region for longitudinal analyses with the amyloid PET ligand [ $^{18}\text{F}$ ]-AV45, as it gives longitudinally more stable results in the normalized tracer uptake (SUVr) compared to commonly applied infratentorial VOIs such as whole cerebellum or BST/pons [13–15]. Based on these reports, we availed ourselves of the multi-center ADNI database

to investigate the association between the apparent rate of amyloid accumulation over a 2-year period and the baseline amyloid burden. Earlier PET studies with [ $^{11}\text{C}$ ]-PiB, the prototypic amyloid tracer, reported that this relationship follows an inverted U-shaped function when infratentorial brain structures are used for tracer uptake normalization [6, 7, 12]. For the current study, we scaled uptake of [ $^{18}\text{F}$ ]-AV45 to WM, and—for the purpose of comparison—to CBL and BST. Analyses were conducted using ADNI data from 144 cognitively normal controls, 225 aMCI patients, and 35 patients with AD.

### Association between $\Delta$ SUVR and baseline SUVr

Our findings confirm an inverted U-shaped relationship between apparent amyloid accumulation rate over time

and baseline amyloid load in case of WM normalization. An inverted U-shaped relationship was also found for the quantification method COMP/BST; however, here, the fitting line implied a washout of amyloid in the longitudinal run at an advanced disease stage, which contradicts the hypothesis that brain amyloid load eventually reaches a plateau [6]. No statistically significant association between amyloid accumulation rate over time and baseline amyloid load was present for COMP/CBL.

The differences in association between apparent amyloid changes over time and amyloid burden at baseline were based on different distributions of  $\Delta$ SUVRs and baseline SUVRs across quantitation methods; this includes the observation that the number of—physiologically less plausible—decliners, i.e., cases in whom the apparent [ $^{18}\text{F}$ ]-AV45 binding declined to follow-up, varied across methods, especially with regard to the distribution across baseline SUVR quartiles. The fewest decliners (in total) were seen for WM, which confirms previous reports of fewer decliners with WM scaling as opposed to cerebellum or pons reference regions [13, 14]. It follows that reference region selection can substantially influence the association between apparent amyloid accumulation rate over time and baseline amyloid burden, at least in the case of [ $^{18}\text{F}$ ]-AV45 (and probably also for other amyloid PET tracers).

#### Association between SUVs at baseline and follow-up

But, what may be the factors accounting for the differences in association between longitudinal SUVR changes and SUVs at baseline across quantification methods? Our results demonstrate that at baseline and follow-up, there are specific differences in the relative contribution of COMP and reference VOI SUVs to SUVs. In detail, we found that the magnitude of SUVs was almost completely determined by the COMP SUV when CBL was used for normalization; in comparison, there was a substantially lower contribution of the COMP SUVs (and thus a higher contribution of the reference VOI SUVs) on SUVs when normalization was performed with BST and especially WM reference regions, a finding that can be linked to the well-known fact that binding of [ $^{18}\text{F}$ ]-AV45 to myelin is high. Our results also show a high degree of association between COMP and WM VOI SUVs—which is higher than that between COMP and the remaining reference VOI SUVs—implying some *functional* coupling between these regions that persists from baseline to follow-up scanning; this inter-regional coupling may explain the more uniform distribution of  $\Delta$ SUVs as a function of baseline SUVs when WM VOI was used for normalization (Fig. 1) as at any given time outlier cortical SUVs are more likely to be paralleled by outlier SUVs in the WM VOI (and vice versa).

We can only speculate about the physiological basis for this coupling between COMP and WM VOIs. Spill-over of the PET

signal between both regions may have substantially accounted for it. However, some (lower) associations also existed between COMP and infratentorial VOI SUVs, which, due to their distance, are unlikely to be caused by spill-over effects. Thus, additional factors may also play an important role, too. One of these factors is the global CBF, which underlies radioligand delivery to the brain. We have earlier shown that a surrogate marker for CBF biased estimation of the specific binding of the dopamine receptor ligand [ $^{18}\text{F}$ ]-fallypride [18]. More pertinently, a study reported highly correlated regional relationships between the relative delivery of the amyloid tracer [ $^{11}\text{C}$ ]-PiB and the relative  $^{15}\text{O}$ -water delivery, a direct surrogate for CBF [19]. Thus, the exceptionally high coupling between COMP and WM SUVs may be additionally caused by CBF effects given that the neocortex and its subjacent WM have a common vascular supply, thus increasing the correlation between COMP and WM tracer delivery. A distinct perfusion of CBL and BST, on the other hand, may explain the lower association between COMP and infratentorial VOI SUVs.

#### Association between VOI SUV changes in the longitudinal run

We found substantial differences in the relative contribution of reference VOI SUV changes to  $\Delta$ SUVs across quantitation methods:  $\Delta$ SUVs were mainly determined by SUV changes within the COMP VOI in the case of COMP/CBL; in contrast, there was a substantially higher impact of reference regions on  $\Delta$ SUVs when BST and WM were applied. Moreover, longitudinal SUV changes within the WM reference tissue showed the highest correlations with those within the COMP VOI suggesting the existence of a *functional* coupling between the neocortex and the subjacent WM also in the longitudinal run. Again, we can only speculate about the physiological basis for this finding. Given that CBF changes are known to occur in aMCI and AD patients with disease progression [20–22], CBF effects—beside PET signal spill-over—may again constitute a relevant confounder. In this regard, van Berckel et al. demonstrated in a [ $^{11}\text{C}$ ]-PiB study that SUVR in AD patients, when determined with the cerebellum for normalization, is sensitive to longitudinal changes of CBF, resulting in increased between-subject variability, especially at follow-up examinations; they link their observation to a longitudinal decrease in tracer delivery to cortical structures relative to the cerebellum due to a reduction in cortical perfusion during the progression of AD [23]. Their explanation is generally plausible as the cerebral cortex is the initial and most affected locus of amyloid pathology, whereas the cerebellum (following the BST) is the last to develop A $\beta$  plaques in the course of AD [10]. From this point of view, the temporal coupling in [ $^{18}\text{F}$ ]-AV45 SUV between COMP and WM may—given the common vascular supply—be in part driven by similarities in perfusion-dependent changes in tracer delivery across these two regions; in contrast,



the reduced association of SUV changes between COMP and infratentorial VOIs may reflect differing changes of relative tracer delivery across these compartments between sessions.

A high degree of temporal CBF and, therefore, SUV coupling between COMP and WM would explain the lower number of negative  $\Delta$ SUVRs for COMP/WM as decreasing COMP SUVs due to a reduction in perfusion are more likely to be counterbalanced by decreasing SUVs in the subjacent WM. Although we have no surrogate marker for CBF changes in the present follow-up amyloid PET study, we think it is plausible that longitudinal CBF decreases in the cortex enhance the creation of spurious SUVR decreases over time when infratentorial regions are applied for normalization, as perfusion decreases in the cortex are imperfectly matched by corresponding changes in the brainstem and especially in the cerebellum. From this it would follow that the increased percentage of SUVR decliners for the 4<sup>th</sup> quartile of baseline SUVRs in the cases of COMP/CBL and COMP/BST does not represent true changes in the specific tracer binding within the cortex and thus a washout of cortical amyloid burden but rather perfusion decreases.

### Correlations with ADAS-Cog13

In the longitudinal run, changes of ADAS-Cog13 scores and SUVRs were statistically significant only for COMP/WM. This finding is comparable with a prior work of Chen et al. who reported significant correlations between SUVR increases and clinical declines for WM referencing only, but not for the cerebellum or the pons [14]. The improved association between clinical data and imaging parameters suggests that PET signal normalization based on WM may represent a more realistic image of the progression of brain amyloidosis. This finding corroborates the theory that compensating for cortical flow changes in the longitudinal run is of particular importance for SUVR determination. Moreover, it weakens the support for inter-regional PET signal spill-over as the predominant factor for the observed COMP/WM coupling given that substantial spill-over effects should tend to decrease the validity of the SUVR and thus of the association between SUVR and clinical data.

### The use of a PVE-corrected COMP VOI scaled by WM

The PVE-corrected data showed some important differences in comparison with the PVEC-free COMP/WM method. First, we observed that the already low total number of SUVR decliners for COMP/WM (131 or 32%) further decreased for COMP\_PVEC/WM (101 or 25%); there was also a relatively lower proportion of SUVR decliners for the 4<sup>th</sup> quartile of the corresponding baseline SUVR levels (4/18). The decreased number of SUVR decliners was associated with greater increases for COMP\_PVEC SUVs over time, which propagated to a higher impact of the COMP\_PVEC configuration on the corresponding  $\Delta$ SUVRs. Accordingly, the association

between  $\Delta$ SUVR and baseline SUVR was best characterized by a logarithmically increasing function in this case, a finding that does not necessarily conflict with a U-shaped association, but may rather indicate that increasing cortical amyloid burden persists for a longer period before it eventually stops. We attribute this difference in association between  $\Delta$ SUVR and baseline SUVR as a consequence of the correction for progression of cortical atrophy [24], which was indeed found to be significant between sessions in the current study population. Second, in comparison with COMP/WM, the coupling between COMP\_PVEC and WM SUVs decreased within each session (baseline:  $r = 0.78$  to  $r = 0.56$ ; follow-up:  $r = 0.79$  to  $r = 0.57$ ), and also over time ( $r = 0.94$  to  $r = 0.67$ ). This is consistent with the expectation that signal spill-over between the cortex and subjacent WM indeed influenced the PVEC-free analysis. Nonetheless, the degree of inter-regional coupling remained relatively high after the correction (correlations between COMP\_PVEC and CBL/BST decreased to  $r < 0.20$ , data not shown here), further supporting the notion that inter-regional changes in perfusion and tracer delivery effects may be of substantial importance. Third, correlations with ADAS-Cog13 increased for COMP\_PVEC/WM, especially in the longitudinal run, demonstrating that correction of COMP SUVs for progressive atrophy may substantially improve the association between SUVR-based quantification of amyloid burden and cognitive performance.

### Limitations

We used a standard PET imaging protocol with acquisition during 50–70 min after [<sup>18</sup>F]-AV45 application. Our hypothesis that CBF changes have a substantial effect on the measured SUVs and thus on the association between  $\Delta$ SUVR and SUVR at baseline could be tested through complete dynamic PET acquisitions, with initial tracer uptake/delivery serving as a surrogate for CBF. The realization of such an approach, however, is hardly feasible in case of large-scale multi-center studies.

The progression of atrophy of brain structures observed in all tested VOIs in the current study emerges as a significant factor in semi-quantitative analyses of amyloid burden. We show that PVEC of the COMP VOI, which accommodates the cortical atrophy, has a substantial effect on the results. In this context, it will be of great importance for future research to extend the use of atrophy correction also to reference regions including WM, which should afford a better understanding of the definitive association between longitudinal SUVR changes and SUVR at baseline.

We note that cerebral binding of the moderately lipophilic [<sup>18</sup>F]-AV45 in WM has been reported to be a predominantly non-specific process [2, 4, 13]. However, there may also be a specific binding component, possibly to amyloid, in lipid-rich WM regions [25]; when present, this component would additionally bias the apparent association between COMP and

WM SUVs. However, the presently available data analysis methods do not support a rigorous examination of the consequences of this possible factor for the quantitation of amyloid burden in the cortex. Finally, present PET results with [<sup>18</sup>F]-AV45 may not be directly comparable to earlier reports with [<sup>11</sup>C]-PiB, especially given the differing proclivities of that tracer for non-specific binding in WM.

## Conclusion

The current work shows that the association between the rate of amyloid accumulation over time and the baseline amyloid burden follows an inverted U-shaped time course for WM normalization with [<sup>18</sup>F]-AV45. However, reference region selection is of paramount importance on this association, which is a key issue in designing longitudinal intervention studies. We find regional and temporal correlations in [<sup>18</sup>F]-AV45 SUVs, which are more pronounced between COMP and WM than between COMP and CBL/BST VOIs. We attribute this coupling mainly to tracer delivery effects mediated by perfusion, especially in the longitudinal run. Due to the plausible covariance of CBF in the cortical mantle and underlying WM, we suggest that SUVR relative to WM may be more robust to changes in CBF and thus fitter for sensitive detection of amyloid accumulation in intervention PET studies with [<sup>18</sup>F]-AV45. This hypothesis seems to be corroborated by an improved association between imaging and clinical data. Our results for the PVE-corrected data do not contradict the inverted U-shaped association, but rather imply that adjustment of SUV measurements for atrophy is beneficial for quantitation, and should certainly be further elucidated in future studies.

**Acknowledgements** Language editing was provided by Inglewood Biomedical Editing. Data collection and sharing for this project was funded by the Alzheimer's Disease Neuroimaging Initiative (ADNI; National Institutes of Health grant U01 AG024904) and DOD ADNI (Department of Defense award number W81XWH-12-2-0012). ADNI is funded by the National Institute on Aging, the National Institute of Biomedical Imaging and Bioengineering, and through generous contributions from the following: AbbVie, Alzheimer's Association; Alzheimer's Drug Discovery Foundation; Araclon Biotech; BioClinica, Inc.; Biogen; Bristol-Myers Squibb Company; CereSpir, Inc.; Cogstate; Eisai Inc.; Elan Pharmaceuticals, Inc.; Eli Lilly and Company; EuroImmun; F. Hoffmann-La Roche Ltd and its affiliated company Genentech, Inc.; Fujirebio; GE Healthcare; IXICO Ltd.; Janssen Alzheimer Immunotherapy Research & Development, LLC.; Johnson & Johnson Pharmaceutical Research & Development LLC.; Lumosity; Lundbeck; Merck & Co., Inc.; Meso Scale Diagnostics, LLC.; NeuroRx Research; Neurotrack Technologies; Novartis Pharmaceuticals Corporation; Pfizer Inc.; Piramal Imaging; Servier; Takeda Pharmaceutical Company; and Transition Therapeutics. The Canadian Institutes of Health Research is providing funds to support ADNI clinical sites in Canada. Private sector contributions are facilitated by the Foundation for the National Institutes of Health ([www.fnih.org](http://www.fnih.org)). The grantee organization is the Northern California Institute for Research and Education, and the study is coordinated by the Alzheimer's

Therapeutic Research Institute at the University of Southern California. ADNI data are disseminated by the Laboratory for Neuro Imaging at the University of Southern California.

## Compliance with ethical standards

**Conflict of interest** The authors declare that they have no conflict of interest.

**Ethical approval** All procedures described in the study were approved by the institutional review boards of each participating institution and were in accordance with the 1964 Helsinki Declaration and its later amendments.

**Informed consent** Informed consent was obtained from all individual participants included in the study.

## References

1. Ikonomic MD, Klunk WE, Abrahamson EE, Mathis CA, Price JC, Tsopelas ND, et al. Post-mortem correlates of in vivo PiB-PET amyloid imaging in a typical case of Alzheimer's disease. *Brain*. 2008;131:1630–45. doi:10.1093/brain/awn016.
2. Camus V, Payoux P, Barre L, Desgranges B, Voisin T, Tauber C, et al. Using PET with 18F-AV-45 (florbetapir) to quantify brain amyloid load in a clinical environment. *Eur J Nucl Med Mol Imaging*. 2012;39:621–31. doi:10.1007/s00259-011-2021-8.
3. Joshi AD, Pontecorvo MJ, Clark CM, Carpenter AP, Jennings DL, Sadowsky CH, et al. Performance characteristics of amyloid PET with florbetapir F 18 in patients with alzheimer's disease and cognitively normal subjects. *J Nucl Med*. 2012;53:378–84. doi:10.2967/jnumed.111.090340.
4. Wong DF, Rosenberg PB, Zhou Y, Kumar A, Raymont V, Ravert HT, et al. In vivo imaging of amyloid deposition in Alzheimer disease using the radioligand 18F-AV-45 (florbetapir [corrected] F 18). *J Nucl Med*. 2010;51:913–20. doi:10.2967/jnumed.109.069088.
5. Dubois B, Feldman HH, Jacova C, Dekosky ST, Barberger-Gateau P, Cummings J, et al. Research criteria for the diagnosis of Alzheimer's disease: revising the NINCDS-ADRDA criteria. *Lancet Neurol*. 2007;6:734–46. doi:10.1016/S1474-4422(07)70178-3.
6. Jack Jr CR, Wiste HJ, Lesnick TG, Weigand SD, Knopman DS, Vemuri P, et al. Brain beta-amyloid load approaches a plateau. *Neurology*. 2013;80:890–6. doi:10.1212/WNL.0b013e3182840bbe.
7. Villemagne VL, Burnham S, Bourgeat P, Brown B, Ellis KA, Salvado O, et al. Amyloid beta deposition, neurodegeneration, and cognitive decline in sporadic Alzheimer's disease: a prospective cohort study. *Lancet Neurol*. 2013;12:357–67. doi:10.1016/S1474-4422(13)70044-9.
8. Fleisher AS, Chen K, Liu X, Ayutyanont N, Roontiva A, Thiyyagura P, et al. Apolipoprotein E epsilon4 and age effects on florbetapir positron emission tomography in healthy aging and Alzheimer disease. *Neurobiol Aging*. 2013;34:1–12. doi:10.1016/j.neurobiolaging.2012.04.017.
9. Doraiswamy PM, Sperling RA, Coleman RE, Johnson KA, Reiman EM, Davis MD, et al. Amyloid-beta assessed by florbetapir F 18 PET and 18-month cognitive decline: a multicenter study. *Neurology*. 2012;79:1636–44. doi:10.1212/WNL.0b013e3182661f74.
10. Thal DR, Beach TG, Zantette M, Heurling K, Chakrabarty A, Ismail A. [(18F)]flutemetamol amyloid positron emission tomography in

- preclinical and symptomatic Alzheimer's disease: specific detection of advanced phases of amyloid-beta pathology. *Alzheimers Dement*. 2015;11:975–85. doi:10.1016/j.jalz.2015.05.018.
11. Barthel H, Gertz HJ, Dresel S, Peters O, Bartenstein P, Buerger K, et al. Cerebral amyloid-beta PET with florbetaben (18F) in patients with Alzheimer's disease and healthy controls: a multicentre phase 2 diagnostic study. *Lancet Neurol*. 2011;10:424–35. doi:10.1016/S1474-4422(11)70077-1.
  12. Villain N, Chetelat G, Grassiot B, Bourgeat P, Jones G, Ellis KA, et al. Regional dynamics of amyloid-beta deposition in healthy elderly, mild cognitive impairment and Alzheimer's disease: a voxelwise PiB-PET longitudinal study. *Brain*. 2012;135:2126–39. doi:10.1093/brain/aws125.
  13. Landau SM, Fero A, Baker SL, Koeppe R, Mintun M, Chen K, et al. Measurement of longitudinal beta-amyloid change with 18F-florbetapir PET and standardized uptake value ratios. *J Nucl Med*. 2015;56:567–74. doi:10.2967/jnumed.114.148981.
  14. Chen K, Roontiva A, Thiyyagura P, Lee W, Liu X, Ayutyanont N, et al. Improved power for characterizing longitudinal amyloid-beta PET changes and evaluating amyloid-modifying treatments with a cerebral white matter reference region. *J Nucl Med*. 2015;56:560–6. doi:10.2967/jnumed.114.149732.
  15. Brendel M, Hogenauer M, Delker A, Sauerbeck J, Bartenstein P, Seibyl J, et al. Improved longitudinal [(18)F]-AV45 amyloid PET by white matter reference and VOI-based partial volume effect correction. *NeuroImage*. 2015;108:450–9. doi:10.1016/j.neuroimage.2014.11.055.
  16. Hammers A, Allom R, Koeppe MJ, Free SL, Myers R, Lemieux L, et al. Three-dimensional maximum probability atlas of the human brain, with particular reference to the temporal lobe. *Hum Brain Mapp*. 2003;19:224–47. doi:10.1002/hbm.10123.
  17. Akaike H. Information theory and an extension of the maximum likelihood principle. In: Petrov BN, Csaki F, editors *Second International Symposium on Information Theory*; Budapest Akademiai Kiado. 1973;pp. 267–81.
  18. Cumming P, Xiong G, la Fougere C, Rominger A, Bartenstein P, Buchholz HG, et al. Surrogate markers for cerebral blood flow correlate with [(1)(8)F]-fallypride binding potential at dopamine D(2/3) receptors in human striatum. *Synapse*. 2013;67:199–203. doi:10.1002/syn.21630.
  19. Chen YJ, Rosario BL, Mowrey W, Laymon CM, Lu X, Lopez OL, et al. Relative 11C-PiB delivery as a proxy of relative CBF: quantitative evaluation using single-session 15O-water and 11C-PiB PET. *J Nucl Med*. 2015;56:1199–205. doi:10.2967/jnumed.114.152405.
  20. Sojkova J, Beason-Held L, Zhou Y, An Y, Kraut MA, Ye W, et al. Longitudinal cerebral blood flow and amyloid deposition: an emerging pattern? *J Nucl Med*. 2008;49:1465–71. doi:10.2967/jnumed.108.051946.
  21. Alegret M, Cuberas-Borros G, Vinyes-Junque G, Espinosa A, Valero S, Hernandez I, et al. A two-year follow-up of cognitive deficits and brain perfusion in mild cognitive impairment and mild Alzheimer's disease. *J Alzheimer's Dis : JAD*. 2012;30:109–20. doi:10.3233/JAD-2012-111850.
  22. Nishimura T, Hashikawa K, Fukuyama H, Kubota T, Kitamura S, Matsuda H, et al. Decreased cerebral blood flow and prognosis of Alzheimer's disease: a multicenter HMPAO-SPECT study. *Ann Nucl Med*. 2007;21:15–23.
  23. van Berckel BN, Ossenkoppele R, Tolboom N, Yaqub M, Foster-Dingley JC, Windhorst AD, et al. Longitudinal amyloid imaging using 11C-PiB: methodologic considerations. *J Nucl Med*. 2013;54:1570–6. doi:10.2967/jnumed.112.113654.
  24. Rullmann M, Dukart J, Hoffmann KT, Luthardt J, Tjepolt S, Patt M, et al. Partial-volume effect correction improves quantitative analysis of 18F-Florbetaben beta-Amyloid PET Scans. *J Nucl Med*. 2016;57:198–203. doi:10.2967/jnumed.115.161893.
  25. Nemmi F, Saint-Aubert L, Adel D, Salabert AS, Pariente J, Barbeau EJ, et al. Insight on AV-45 binding in white and grey matter from histogram analysis: a study on early Alzheimer's disease patients and healthy subjects. *Eur J Nucl Med Mol Imaging*. 2014;41:1408–18. doi:10.1007/s00259-014-2728-4.